

# Phytofabrication of Magnetite Nanoparticles from *Piper betle* (L.) var. Mysore and Evaluation of Anti-Breast Cancer Potentials

Ravikant Shekhar, Harischandra Sripathy Prakash, Nagaraja Geetha\*

Department of Studies in Biotechnology, University of Mysore, Mysore, Karnataka, INDIA.

## ABSTRACT

**Background:** Breast cancer is a predominant disease around the world, with early diagnosis aiding in reducing the spread and recurrence. Plant-mediated nanoparticles have shown promising results in treatment. The current study aimed to synthesize Magnetite Nanoparticles (MNPs) utilizing *Piper betle* var. Mysuru extract and evaluate its anti-breast cancer potentials. **Materials and Methods:** The green synthesis included  $\text{Fe}^{3+}$  and  $\text{Fe}^{2+}$  in a 2:1 proportion, with crude ethyl acetate extract as a reducing, stabilizing, capping, and tailing agent. The MNPs were characterized utilizing UV-vis spectrometry, SEM, EDX, XRD, FTIR, and DLS for various properties like size, crystal structures, presence of functional groups, surface topologies, etc. **Results:** The diameter of the newly synthesized nanoparticle was 90 nm in diameter, with a face-centered crystal lattice with different phytochemicals like alcohol, phenols, alkanes, etc. The cytotoxicity assay showed  $\text{IC}_{50}$  values of Doxorubicin, plant extract, and MNPs to be  $16.77 \pm 0.56 \mu\text{g/mL}$ ,  $26.07 \pm 3.14 \mu\text{g/mL}$ , and  $12.35 \pm 2.47 \mu\text{g/mL}$ , respectively. The hemolytic assay showed 8.8% and 12.28% hemolytic activity with plant extract and MNPs, respectively. **Conclusion:** The MNPs' affordability, Eco-friendliness, and ease of synthesis make them ideal candidates for upscale synthesis to be used as an active drug molecule against breast cancer.

**Keywords:** Magnetite nanoparticles, Phytofabrication, FTIR, XRD, DLS, MTT assay, Hemolytic Assay.

## Correspondence:

**Prof. Nagaraja Geetha**

Department of Studies in Biotechnology,  
University of Mysore, Manasagangotri  
Campus, Mysore-570006, Karnataka,  
INDIA.

Email: geetha@appbot.uni-mysore.ac.in

**Received:** 01-05-2025;

**Revised:** 30-06-2025;

**Accepted:** 18-08-2025.

## INTRODUCTION

Cancer is considered among the deadliest diseases with a high death rate occurring worldwide. The risk associated with the disease is profusely growing cells which can potentially migrate to different regions of the body causing various diseases.<sup>1</sup> BC is the most common type of cancer among females with around 25% likely to occur more than other cancer types, and can be cured based on the early diagnosis. Early diagnosis makes the disease treatable but there is always a risk of reoccurrence even after being fully treated.<sup>2,3</sup> BC is regarded as the most commonly diagnosed cancer in the world, even then the estimated death of around 6,85,000 individuals in the year 2020 particularly among developing countries, corresponding to 16% of total deaths caused by cancer.<sup>4</sup> BC emerges in the epithelial cells of ducts or lobes in the breast's glandular tissue.<sup>5</sup>

The cancer cells can easily develop resistance to the administered drug because of numerous genetic and epigenetic factors, making the treatment very difficult leaving behind only methods like surgery, chemotherapy, and radiation. One approach to overcome this resistance is the administration of combinational drugs for the molecular pathways exclusively targeting the growth and survival of the cancerous cells.<sup>6,7</sup> Further, the utilization of novel therapeutic drugs in the combination has shown promising results by enhancing the survival rates of the patients, and success in case of delayed treatment. It also has a reduction in the reappearance of cancer and the development of resistance to chemotherapy.<sup>8</sup>

Secondary metabolites are the product of the alkaloid and phenylpropanoid pathways, produced by the plants to be better adapted to environmental stress. These metabolites have a huge impact on the plant and possess high pharmaceutical value as they exhibit properties like anti-oxidant, anti-inflammatory, anti-diabetic, etc. Many of these metabolites show cytotoxic effects, anti-angiogenesis, and apoptotic properties which can be exploited for the prevention of Cancer.<sup>9</sup> *Piper betle* L. (*Piperaceae*) is a Pan-Asiatic medicinal plant rich in bioactive Phyto compounds such as hydroxychavicol, eugenol, isoeugenol, anethole, etc.<sup>10</sup> The betel leaf which is native to South Asia including India, Indonesia, and Malaysia, is commonly used as a mouth freshener and holds



DOI: 10.5530/ijper.20261603

### Copyright Information :

Copyright Author (s) 2026 Distributed under  
Creative Commons CC-BY 4.0

Publishing Partner : Manuscript Technomedia. [www.mstechnomedia.com]

important socio-economical values.<sup>11,12</sup> The Mysuru variety of *Piper betle* has a heart-shaped leaf and is known for its unique hot and spicy taste with a smooth texture is cultivated in and around the Mysuru district of Karnataka, India, and got the GI tag in April 2006-2007.<sup>13</sup>

Iron oxides naturally form magnetite in the natural crystalline cubical structure whose central position is occupied by Ferrous and Ferric ions. The nano range structure of magnetite particles has various unique properties which have attracted scientists for its implementation in particular medical fields for the efficient treatment of several ailments. Magnetite Nanoparticles (MNPs) occur in various forms, including cubes, rods, disks, tubes, plates, hexagons, octahedrons, tetrahedrons, octopods, tetrapods, rings, flowers, etc.<sup>14,15</sup> MNPs implementation in various fields depends on their physical and chemical properties which are governed primarily based on different factors like shape size and size distribution. These magnetites at specific temperatures show a peculiar property namely supra-magnetism, without being polarized on normal, without any attractive field, when the particle size is very small. The combination of MNPs with controlled size can be utilized in different applications, for example, ferrofluid, rotational shaft fixing, wavering damping, and position detecting.<sup>16-18</sup>

The current study aims for ethyl acetate extract of *Piper betle* var. Mysore-mediated green synthesis of magnetite nanoparticle and checking its potential for efficient utilization as an active drug molecule for anti-breast cancer.

## MATERIALS AND METHODS

### Materials

Ferric Chloride and Ferrous Sulfate were procured from Thermo Fisher Scientific, India. Doxorubicin and MTT were procured from Sigma India. DMEM was procured from Hi-Media, Mumbai, India. Methanol and Ethyl acetate were procured from SD-Fine Chemical Ltd., Mumbai, India. All chemicals used for the study were of analytical grade.

### Plant Sample Collection and Preparation

Fresh leaves of *Piper betle* L. var. Mysuru were collected from the Horticulture Division of the University of Mysore, Mysuru (Karnataka), washed with normal water and deionized water, and kept for drying at room temperature.

The leaves were made to powder by grinding and were subjected to extraction in the Soxhlet apparatus using ethyl acetate as solvent. This crude extract was concentrated by the utilizing solvent evaporation method in a rotary evaporator (Heidolph, Germany). This concentrate was dissolved in methanol in varying concentrations for different assays.<sup>19</sup>

### Synthesis of MNPs

MNPs were synthesized using the above-prepared plant crude extract of *Piper betle* var. Mysuru. MNP synthesis was started with the preparation of Ferric chloride and Ferrous Sulfate solution by dissolving it in a 2:1 ratio. The extract (10 mg/mL) was added to the above-prepared solution gently with continuous stirring at 25°C using a magnetic stirrer. The pH was adjusted to 10 by using an ammonium hydroxide solution. The solution was incubated for 1 hour with continuous stirring for homogenization. The newly synthesized MNPs were collected with the application of an external magnet. The MNPs were washed multiple times with water, followed by ethanol, and were dried at room temperature.<sup>20</sup>

### Characterization of MNPs

#### UV-vis Spectrophotometer

The dried nanoparticle was homogenized using a sonicator at 40% amplitude with a pulse on/off for 5/5 sec for 3 hr in methanol.<sup>21</sup> The homogenized MNPs were subjected to various characterization techniques.

UV-vis Spectrophotometer (Hitachi-U-3900, Japan) was utilized for the characterization of newly synthesized MNPs by performing the wavelength scan (200 nm to 800 nm) to find out the characteristic peak associated with MNPs.<sup>22</sup>

#### Scanning Electron Microscopy and Energy-Dispersive X-ray analysis

The surface topology and the elemental constituent were estimated utilizing a Scanning Electron Microscope (SEM) (Hitachi-S-3400N, Japan) working at 5kV vacuum conditions combined with Energy Dispersive X-ray (EDX).<sup>23</sup>

#### DLS and Zeta potential analysis

Dynamic Light Scattering (DLS) was used for the size distribution, dispersive index, and Zeta potential of synthesized MNPs.<sup>24,25</sup> The analysis was carried out by dissolving the 1mg of dried nanoparticle in 2 mL of distilled water and was subjected to DLS analysis (Microtrac Molecule Size Analyzer).

#### XRD analysis

The crystal structure along with the crystal lattice of the synthesized MNPs was analyzed by using X-ray Diffraction (XRD).<sup>26</sup>

#### FTIR analysis

The presence of various functional groups was determined by using Fourier Transform Infra-Red Spectroscopy (FTIR) which is responsible for the synthesis as well as associated with the activity of MNPs.<sup>26</sup>

## Cytotoxicity Assay

Cytotoxicity assay was performed using MCF-7 cell lines (ATCC-HBT22), which is an Estrogen Receptor (ER) positive with Her2 negative cell lines for breast cancer. On a pre-labeled 96-well plate with sample/control drug (Doxorubicin) in varying concentrations (1.56-100 µg/mL). 100 µL of cell suspension (50,000 cells/well) was added and the plate was incubated at 37°C for 24 hr. After incubation, the monolayer formed was washed with Dulbecco's Modified Eagle Medium (DMEM), while the supernatant was discarded. After incubation, the sample/control drug was discarded and 100 µL of MTT reagent (4 mg/10 mL in PBS) was added and was incubated for 4 hr at 37°C. The supernatant was discarded, and DMSO (100 µL) was added with plates gently shaken for the solubilizing formazan crystals. The absorbance was recorded at 590 nm using a multimode plate reader, (Spectra max i3X, and Molecular devices).<sup>27</sup> The growth inhibition percentage was calculated using the formula and the IC<sub>50</sub> values were generated from the dose-dependent curves.

$$\% \text{ Inhibition} = \frac{(\text{OD of control} - \text{OD of sample})}{(\text{OD of Control})} \times 100$$

## Hemolytic Assay

The biocompatibility of the samples with the RBC was checked through hemolytic assay using the protocol described by Sæbø *et al.*,<sup>28</sup> with modifications. The assay was performed using 5 mL of blood collected in K2 EDTA tubes from the healthy individual (without Non-Steroidal Anti-Inflammatory Drugs (NSAIDs), at least two weeks before collection of blood), centrifuged at 3000 rpm for 5 min, the supernatant was discarded and the erythrocytes were washed thrice with Phosphate Buffer Saline (PBS). The pellets were resuspended in PBS (1:100). The suspended erythrocytes were stored at 4°C and were used within 6 hr. 50 µL of uniformly suspended erythrocytes were taken and mixed with an equal volume of samples (25- 150 µg/mL), triton X-100 was used as a positive control to obtain 100% hemolysis and PBS as a negative control. The tubes were incubated at 37°C for 60 min, and centrifuged for 3 min at 300 rpm. The absorbance of the supernatant was measured at 540 nm. The Haemolysis percentage was calculated using the following formula.

$$\% \text{ Hemolysis} = \frac{OD(\text{test}) - OD(\text{negative control})}{(OD(\text{positive control}) - OD(\text{negative control}))} \times 100$$

## Statistical Analysis

The assay was replicated thrice and the results were expressed in the form of mean ± standard deviation. Further, the Analysis of Variance (ANOVA) test was carried out using Tukey's method of analysis and for multiple comparisons with a confidence interval of 95% with *p*-value <0.05 as the significance level over IC<sub>50</sub> values of the cytotoxicity assay.

## RESULTS

### Characterization of MNPs

#### UV-vis Spectrophotometer analysis

Upon incubation, the change of color from yellow to black was observed which suggests the synthesis of nanoparticles. The newly synthesized nanoparticles were subjected to the wavelength scan (200-800 nm) using a UV-vis spectrophotometer. In the wavelength scan, a prominent broad peak was observed at a wavelength of 300 nm (Figure 1).

#### SEM and EDX analysis

Direct observation of the MNPs under SEM revealed surface topology and the approximate size of the newly synthesized MNPs. The analysis showed MNP crystals of varying sizes with irregular shapes at different magnifications (3.00K, 4.00K, and 6.00K) (Figures 2 a-c). The size of the MNPs was found to be of varying size ranging between 80-95 nm ranges. The EDX analysis showed the weight percentage and atomic percentage of Fe to be 60.90% and 30.80% respectively of the newly synthesized MNPs (Figure 2d).

#### DLS and Zeta Potential analysis

The DLS analysis was performed in the water as a solvent for the estimation of the particle size distribution of the synthesized MNPs. The DLS analysis showed the size distribution of the MNPs in the water medium, ranging between 50-250 nm in diameter with the maximum particle of size 90 nm (60% of the nanoparticle). The zeta potential value of the MNPs was found

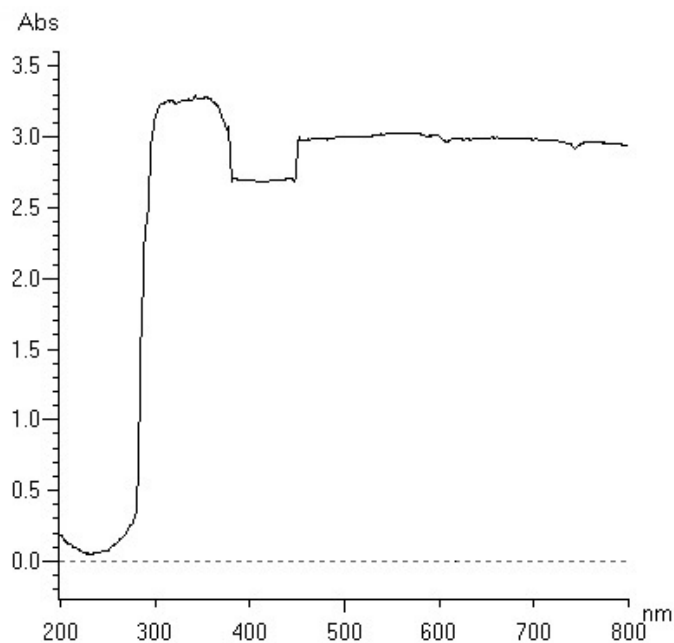


**Figure 1:** UV-vis spectrum for the wavelength scan showing a characteristic peak at 300 nm.

to be -2.1 mV with an overall surface charge to be -0.00159 fC (Figure 3).

### XRD analysis

The crystallinity of synthesized MNPs was investigated using the X-ray Diffraction (XRD) technique. The XRD analysis showed that the MNPs exhibited three distinct peaks at  $2\theta$  values of 35.66, 57.29, and 63.37. All three peaks corresponded to standard Bragg reflections (311), (511), and (440) of face-centered cubic (fcc) lattice (Figure 4).

### FTIR analysis

The spectrum obtained from the FTIR analysis revealed the presence of peaks at different wave numbers with varying intensities suggesting different phytochemicals involved actively in the synthesis and stability of MNPs. The prominent peaks at the wave numbers  $3424.61\text{ cm}^{-1}$ ,  $1401.30\text{ cm}^{-1}$ ,  $631.20\text{ cm}^{-1}$ , and  $562.23\text{ cm}^{-1}$  respectively (Figure 5).

### Cytotoxicity Assay

The cytotoxicity assay (MTT assay) carried out using MCF-7 cell lines showed the anti-breast cancer potential of newly synthesized MNPs. The  $IC_{50}$  value of the standard drug Doxorubicin, Plant

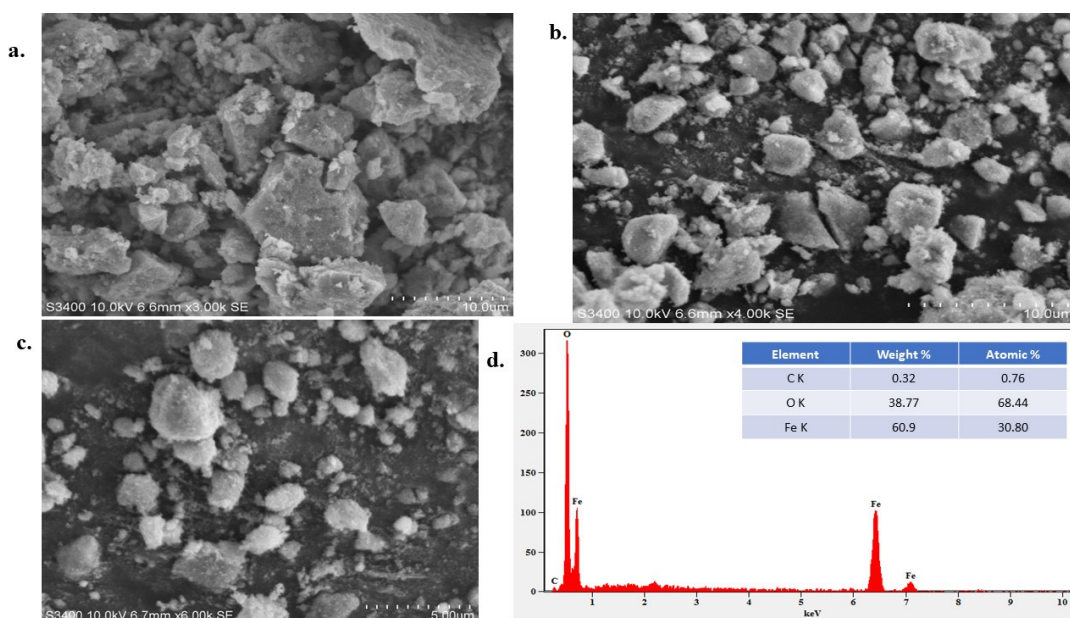


**Figure 2:** SEM image showing the surface topology of MNPs at different magnifications a) 3.00k. b) 4.00k. c) 6.00k and d) EDX showing the presence of Fe with the table containing the weight and atomic percentage.

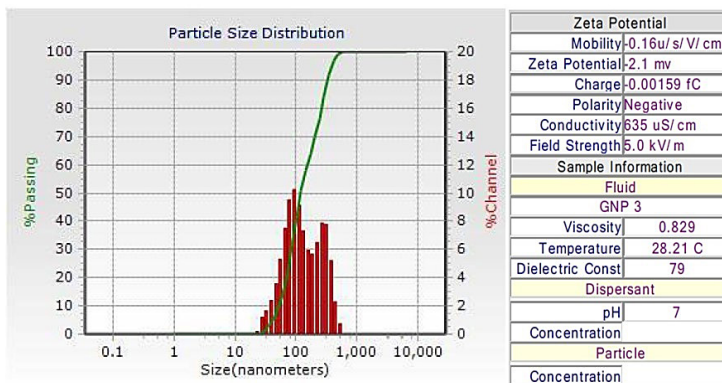


**Figure 3:** DLS showing the presence of higher percentage of the particle having the diameter of 90nm along with the zeta potential and overall surface charge on MNPs.

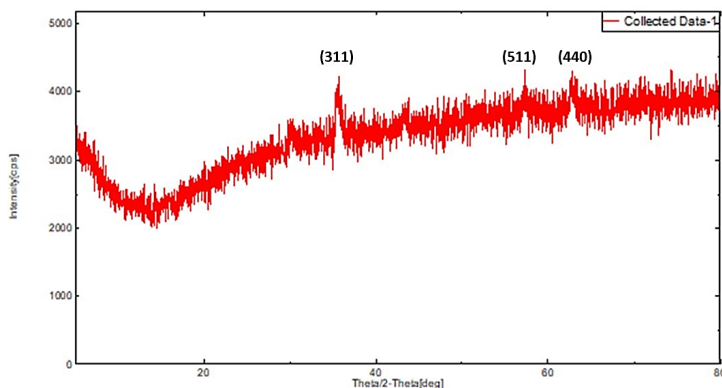


**Figure 4:** XRD pattern showing the peaks at standard Bragg reflections (311), (511), and (440) of fcc lattice forming the diamond cubic structure.

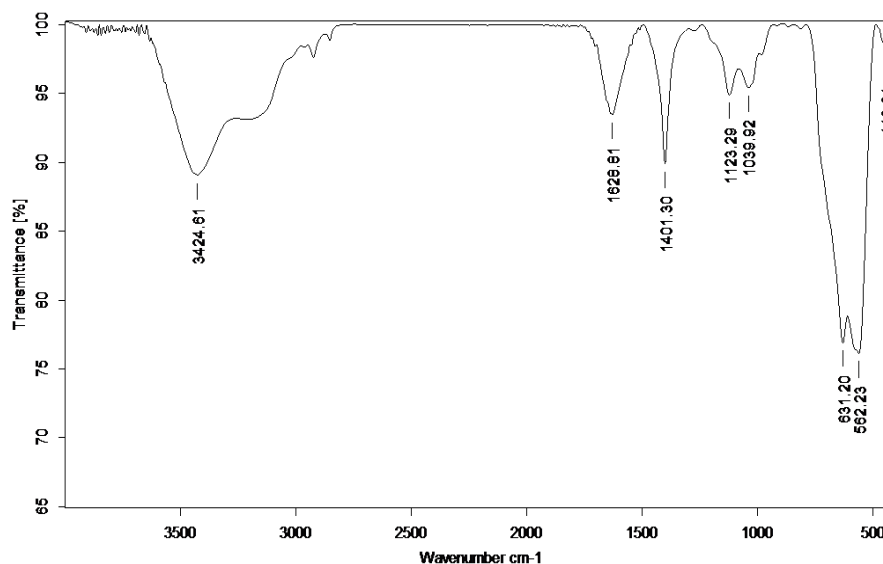


**Figure 5:** The FTIR spectrum of MNPs showing the presence of various phytochemicals at its corresponding peaks.

extract, and MNPs was found to be  $16.77 \pm 0.56 \mu\text{g/mL}$ ,  $26.07 \pm 3.14 \mu\text{g/mL}$  and  $12.35 \pm 2.47 \mu\text{g/mL}$  respectively (Figure 6).

### Hemolytic Assay

The hemolytic assay reveals the percent hemolysis of *Piper betle* var. Mysuru ethyl acetate extract has a hemolysis activity of 8.8% at the higher concentration of  $125 \mu\text{g/mL}$  while the MNPs have a hemolysis activity of 12.28% at  $125 \mu\text{g/mL}$  concentration (Figure 7).

### DISCUSSION

The presence of a broad peak at the 300 nm wavelength suggests that the synthesized nanoparticle is Magnetite Nanoparticles as absorption maxima for the iron oxide shows in the range to

300-320 nm,<sup>29</sup> conforming the synthesized nanoparticle was MNPs.

The DLS assay showed that the medium contain higher size particles which can be attributed towards the formation of aggregated particles in the aqueous medium because of its hydrophobic surface properties.<sup>20</sup>

The XRD resulted in an intense diffraction peak at  $2\theta=35.66$  peak suggesting that the preferred growth orientation of the synthesized nanoparticle was fixed in (311) direction having a face-centered cubic lattice. This refers to molecular-sized crystals arranged in a diamond cubic structure where each atom is bound to neighboring four atoms, forming a tetrahedral structure. This XRD pattern is typical of pure magnetite nanoparticles.<sup>30</sup>

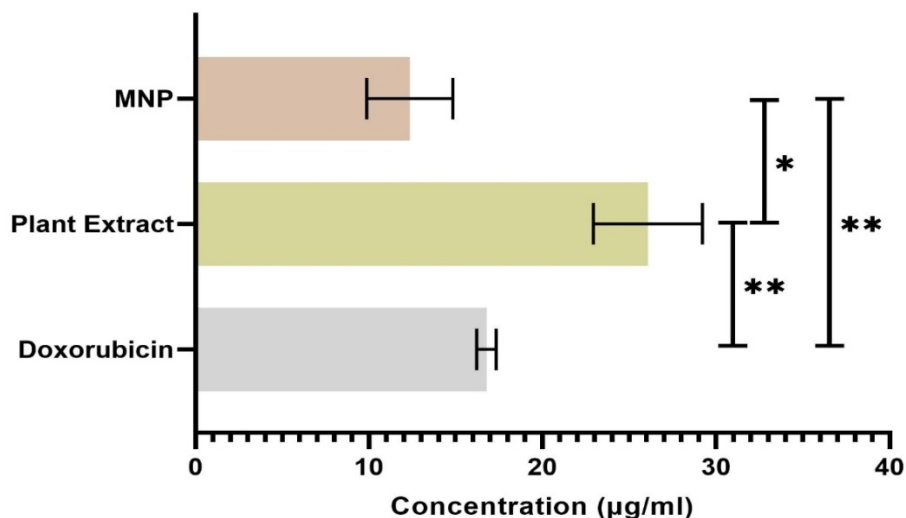


**Figure 6:** The graph showing the IC<sub>50</sub> values for the MTT assay of the Standard, Plant extract and the MNPs. The error bar represents the standard deviation, while \* represents the significant difference between the samples at  $p < 0.05$ .

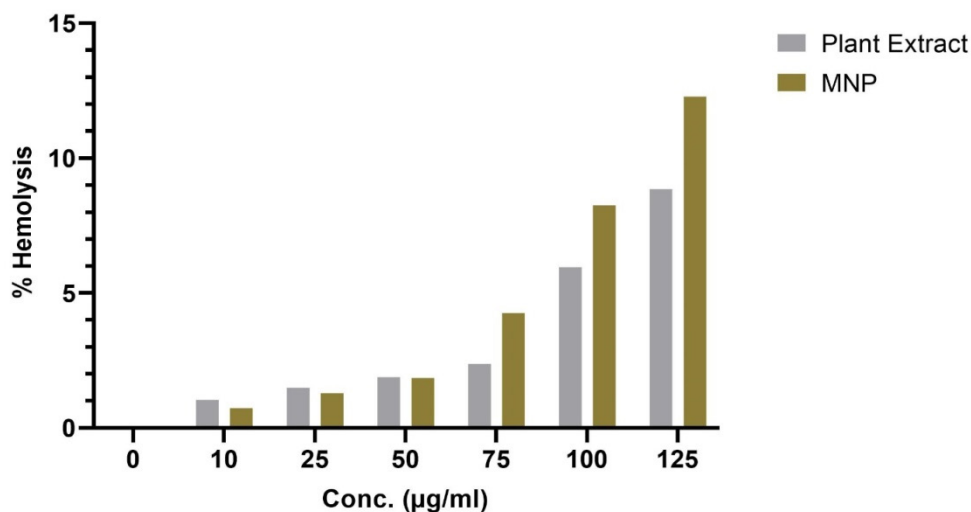


**Figure 7:** The graph showing the percentage haemolysis of the Plant crude extract and MNPs.

The FTIR spectra demonstrated a broad peak along the wave numbers 3200-3550  $\text{cm}^{-1}$  which is attributed to O-H stretching, which arises because of the alcohol and phenolic compounds.<sup>31,32</sup> The peak corresponding to the OH stretching is broader than that of other peaks representing the strong hydrogen bond between the phytochemicals suggesting that the MNPs were capped with the phytoconstituents present.<sup>33,34</sup> The wavenumber 1628.81  $\text{cm}^{-1}$  contributes towards the C=C groups from alkenes,<sup>35</sup> the wavenumber 1401.30  $\text{cm}^{-1}$  constitutes the C-H bending from the alkane group. The wavenumber 1039.92-1123.29  $\text{cm}^{-1}$  is attributed towards C-N stretching of the amine group, while 562.23 -631.20  $\text{cm}^{-1}$  corresponds to C-Cl stretching of halo compounds.<sup>36</sup>

The cytotoxicity assay suggests that the *Piper betle var.* Mysore-mediated MNPs have a better *in vitro* anti-breast cancer

potential than the commonly used drug Doxorubicin. This can be explained as the cytotoxicity of MNPs greatly enhanced with the exposure time, concentration as well as the coating over the nanoparticles. The result also suggests that the *Piper Betle var.* Mysore itself shows some of the anti-breast cancer potentials which are being enhanced to many folds by the nanoparticles.<sup>37,38</sup>

MNPs showed a hemolytic activity of less than 10 % (0-100  $\mu\text{g/mL}$ ) which is considered low hemolysis according to the American Society for Testing and Materials (ASTM), making it safe for long-term circulation in the blood.<sup>39</sup> The Hemolytic assay suggests that MNPs are having greater hemolytic activity over the plant crude extract at the highest concentration (above 10 %). This is attributed to the disruption of the RBC by the MNPs at the targeted site, making it an effective targeted drug molecule

and hence increasing the overall efficacy of the nanoparticle. The results also suggest the hemolytic activity of MNPs is in a dose-dependent fashion.

## CONCLUSION

MNPs which have been synthesized using non-toxic eco-friendly chemicals are inexpensive and can be upscaled easily by utilizing the bioactive metabolites present in the ethyl acetate extract of *Piper betle* as a stabilization as well as for capping and tailing agent. The present study reveals the anti-breast cancer potentials of MNPs, which can be exploited for the preparation of anti-cancer drugs particularly for breast cancer in various formulations such as site-directed subcutaneous injection, oral pills, etc. with the consideration that phyto-fabricated MNPs are having a higher surface to volume ratio and the synthesis is from the natural plant-based sources the application and the utilization of the MNPs are quite safe and have additional benefits over the chemically synthesized drug molecule for having fewer side-effects.

## ACKNOWLEDGEMENT

The authors would like to acknowledge the University Grants Commission (UGC), New Delhi, for the opportunity to carry out the present study. The authors also acknowledge the Department of Studies in Biotechnology, University of Mysore, for providing the infrastructures and basic facilities to carry out the research activity.

## ABBREVIATIONS

**BC:** Breast Cancer; **MNPs:** Magnetite Nanoparticles; **SEM:** Scanning Electron Microscope; **EDX:** Energy Dispersive X-ray; **XRD:** X-ray Diffraction; **FTIR:** Fourier Transform Infrared Spectroscopy; **DLS:** Dynamic Light Scattering; **MTT:** 3-(4,5-dimethylthiazol-2-yl)-2,5-diphenyltetrazolium bromide; **DMEM:** Dulbecco's Modified Eagle Medium; **DMSO:** Dimethyl Sulfoxide; **OD:** Optical Density; **IC<sub>50</sub>:** 50% Inhibitory Concentration; **FCC:** Face-centered Cubic.

## CONFLICT OF INTEREST

The authors declare that the research was conducted in the absence of any commercial or financial relationships that could be construed as a potential conflict of interest.

## FUNDING

The authors would like to express their gratitude to the University Grants Commission (UGC), New Delhi, for providing the BSR-Faculty Fellowship to H.S. Prakash and Research Fellowship to Ravikant Shekhar.

## ETHICAL APPROVAL

The Ethical Approval is not applicable as the cell lines used for the study were Acquired from the Commercial platform (ATCC), it was NOT derived from the primary cell or isolated directly from humans.

## SUMMARY

The study aims to synthesize the Magnetite nanoparticle from the ethyl acetate extract of *Piper betle var. Mysore* and to access its potential to be used as an anti-breast cancer drug. The crucial step towards the efficacy of a nanoparticle is its overall surface properties, size, and charges associated with the stability of the nanoparticle. The synthesized MNPs were characterized using DLS, XRD, and FTIR to determine their size, crystal structures, and functional groups. The synthesized MNPs on testing against MCF-7 cell lines, showed promising cytotoxicity against the cells. Further, the MNPs also show a small amount of hemolytic activity making them suitable for the targeted application of the nanoparticle in the vicinity of the tumor, where it will disrupt the RBCs, thus the synthesized MNPs are very well suited for a potential drug molecule upon scaleup.

## REFERENCES

- Sun J, Wei Q, Zhou Y, Wang J, Liu Q, Xu H. A systematic analysis of FDA-approved anticancer drugs. *BMC Syst Biol.* 2017; 11(Suppl 5).
- Malvia S, Bagadi SA, Dubey US, Saxena S. Epidemiology of breast cancer in Indian women. *Asia Pac J Clin Oncol.* 2017; 13(4): 289-95.
- Harbeck N, Penault-Llorca F, Cortes J, Gnani M, Houssami N, Poortmans P, *et al.* Breast cancer. *Nat Rev Dis Prim [Internet].* 2019; 5(1): 66. Available from: <https://www.nature.com/articles/s41572-019-0111-2>
- Arnold M, Morgan E, Rungay H, Mafra A, Singh D, Laversanne M, *et al.* Current and future burden of breast cancer: Global statistics for 2020 and 2040. *Breast [Internet].* 2022; 66(August):15-23. Available from: <https://doi.org/10.1016/j.breast.2022.08.010>
- WHO. Breast cancer [Internet]. WHO News Room. 2021. p. 5-11. Available from: <https://www.who.int/news-room/fact-sheets/detail/breast-cancer>
- Bundela S, Sharma A, Bisen PS. Potential therapeutic targets for oral cancer: ADM, TP53, EGFR, LYN, CTLA4, SKIL, CTGF, CD70. *PLoS One.* 2014; 9(7).
- Hagerstrand D, Tong A, Schumacher SE, Ilic N, Shen RR, Cheung HW, *et al.* Systematic interrogation of 3q26 identifies TLOC1 and SKIL as cancer drivers. *Cancer Discov.* 2013; 3(9): 1044-57.
- Chakraborty JB, Mahato SK, Joshi K, Shinde V, Rakshit S, Biswas N, *et al.* Hydroxychavicol, a *Piper betle* leaf component, induces apoptosis of CML cells through mitochondrial reactive oxygen species-dependent JNK and endothelial nitric oxide synthase activation and overrides imatinib resistance. *Cancer Sci.* 2012; 103(1): 88-99.
- Ozcan T, Akpınar-Bayazit A, Yılmaz-Ersan L, Delikanlı B. Phenolics in Human Health. *Int J Chem Eng Appl.* 2014; 5(5): 393-6.
- Vinuri S, Gnanam R, Caroline R, Santhanakrishnan VP, Kandavelmani A. Anticancer Potential of Hydroxychavicol Derived from *Piper betle* L: An in Silico and Cytotoxicity Study. *Nutr Cancer [Internet].* 2022; 74(10): 3701-13. Available from: <https://doi.org/10.1080/01635581.2022.2085310>
- Dwivedi V, Tripathi S. Review Study on Potential activity of *Piper betle*. *J Pharmacogn Phytochem.* 2014; 3(4): 93-8.
- Nayaka NMDMW, Sasadara MMV, Sanjaya DA, Yuda PESK, Dewi NLKAA, Cahyaningsih E, *et al.* *Piper betle* (L): Recent review of antibacterial and antifungal properties, safety profiles, and commercial applications. *Molecules.* 2021; 26(8): 1-21.
- Geographical Indications Govt. of India. About Us [Internet]. Available from: <https://pindia.gov.in/about-us-gi.htm>
- Dudchenko N, Pawar S, Perelshtein I, Fixler D. Magnetite Nanoparticles: Synthesis and Applications in Optics and Nanophotonics. *Materials (Basel).* 2022; 15(7).
- Leo D, Alfredo V, Villegas R, Hernandez E, Perez S, Angelica L, *et al.* Synthesis and characterization of magnetite nanoparticles for photocatalysis of nitrobenzene. 2020; 223-35.
- Liu CH, Mao BH, Gao J, Zhang S, Gao X, Liu Z, *et al.* Size-controllable self-assembly of metal nanoparticles on carbon nanostructures in room-temperature ionic liquids by

- simple sputtering deposition. Carbon N Y [Internet]. 2012; 50(8): 3008-14. Available from: <http://dx.doi.org/10.1016/j.carbon.2012.02.086>
17. IET Nanobiotechnology-2019-Aguilar-Mendez-Synthesis and characterisation of magnetite nanoparticles using gelatin and.pdf.
  18. Phumying S, Labuayai S, Thomas C, Amornkitbamrung V, Swatsitang E, Maensiri S. Aloe vera plant-extracted solution hydrothermal synthesis and magnetic properties of magnetite (Fe<sub>3</sub>O<sub>4</sub>) nanoparticles. Appl Phys A Mater Sci Process. 2013; 111(4): 1187-93.
  19. Shekhar R, MC M, CJ S, HS P, Nagaraja G. *In vitro* anti-lipid peroxidation and anti-Candidal potentials of different betel leaf varieties. J Med Plants Stud [Internet]. 2022 Jul 1; 10(4): 140-9. Available from: <https://www.plantsjournal.com/archives/?year=2022&vol=10&issue=4&part=B&ArticleId=1446>
  20. Abdullah M, Atta A, Allohedan H, Alkhatlan H, Khan M, Ezzat A. Green Synthesis of Hydrophobic Magnetite Nanoparticles Coated with Plant Extract and Their Application as Petroleum Oil Spill Collectors. Nanomaterials [Internet]. 2018; 8(10): 855. Available from: <http://www.mdpi.com/2079-4991/8/10/855>
  21. Wroblewski C, Volford T, Martos B, Samoluk J, Martos P. High Yield Synthesis and Application of Magnetite Nanoparticles (Fe<sub>3</sub>O<sub>4</sub>). Magnetochemistry [Internet]. 2020; 6(2): 22. Available from: <https://www.mdpi.com/2312-7481/6/2/22>
  22. Behzadi S, Ghasemi F, Ghalkhani M, Ashkarran AA, Akbari SM, Pakpour S, *et al.* Determination of nanoparticles using UV-vis spectra. Nanoscale. 2015; 7(12): 5134-9.
  23. Gniadek M, Dąbrowska A. The marine nano- and microplastics characterisation by SEM-EDX: The potential of the method in comparison with various physical and chemical approaches. Mar Pollut Bull. 2019; 148: 210-6.
  24. Babick F. Dynamic light scattering (DLS). In: Characterization of Nanoparticles. Elsevier; 2020. p. 137-72.
  25. Bhattacharjee S. DLS and zeta potential-What they are and what they are not? J Control Release. 2016; 235: 337-51.
  26. Balakrishnan GS, Rajendran K, Kalirajan J. Microbial synthesis of magnetite nanoparticles for arsenic removal. J Appl Biol Biotechnol [Internet]. 2020; 8(3): 70-5. Available from: [https://jabonline.in/abstract.php?article\\_id=456&sts=2](https://jabonline.in/abstract.php?article_id=456&sts=2)
  27. Pant A. MTT Assay. Dict Toxicol. 2024; 6597: 662.
  28. Sæbø IP, Bjørås M, Franzyk H, Helgesen E, Booth JA. Optimization of the Hemolysis Assay for the Assessment of Cytotoxicity. Int J Mol Sci. 2023; 24(3).
  29. Lyon JL, Fleming DA, Stone MB, Schiffer P, Williams ME. Synthesis of Fe Oxide Core/Au Shell Nanoparticles by Iterative Hydroxylamine Seeding. Nano Lett [Internet]. 2004; 4(4): 719-23. Available from: <https://pubs.acs.org/doi/10.1021/nl035253f>
  30. Torres-Gómez N, Nava O, Argueta-Figueroa L, García-Contreras R, Baeza-Barrera A, Vilchis-Nestor AR. Shape Tuning of Magnetite Nanoparticles Obtained by Hydrothermal Synthesis: Effect of Temperature. J Nanomater [Internet]. 2019 Feb 7; 2019: 1-15. Available from: <https://www.hindawi.com/journals/jnm/2019/7921273/>
  31. Singh TP, Chauhan G, Agrawal RK, Mendiratta SK. *In vitro* study on antimicrobial, antioxidant, FT-IR and GC-MS/MS analysis of *Piper betle* L. leaves extracts. J Food Meas Charact [Internet]. 2019; 13(1): 466-75. Available from: <http://link.springer.com/10.1007/s11694-018-9960-8>
  32. Punuri JB, Sharma P, Sibyala S, Tamuli R, Bora U. *Piper betle*-mediated green synthesis of biocompatible gold nanoparticles. Int Nano Lett [Internet]. 2012; 2(1): 18. Available from: <https://link.springer.com/10.1186/2228-5326-2-18>
  33. Duan H, Wang D, Li Y. Green chemistry for nanoparticle synthesis. Chem Soc Rev [Internet]. 2015; 44(16): 5778-92. Available from: <https://xlink.rsc.org/?DOI=C4CS00363B>
  34. Ovais M, Khalil AT, Raza A, Khan MA, Ahmad I, Islam NU, *et al.* Green Synthesis of Silver Nanoparticles Via Plant Extracts: Beginning a New Era in Cancer Theranostics. Nanomedicine [Internet]. 2016; 11(23): 3157-77. Available from: <https://www.tandfonline.com/doi/full/10.2217/nmm-2016-0279>
  35. Wulandari L, Retnaningtyas Y, Nuri, Lukman H. Analysis of Flavonoid in Medicinal Plant Extract Using Infrared Spectroscopy and Chemometrics. J Anal Methods Chem [Internet]. 2016; 2016: 1-6. Available from: <http://www.hindawi.com/journals/jamc/2016/4696803/>
  36. Badmapriya D, Asharani I. Dye degradation studies catalysed by green synthesized iron oxide nanoparticles. Int J ChemTech Res. 2016; 9(6): 409-16.
  37. Saranya S, Vijayarani K, Pavithra S, Raihana N, Kumanan K. *In vitro* cytotoxicity of Zinc oxide, iron oxide and copper nanopowders prepared by green synthesis. Toxicol. Rep. 2017; 4: 427-30.
  38. Peng Q, Huo D, Li H, Zhang B, Li Y, Liang A, *et al.* ROS-independent toxicity of Fe<sub>3</sub>O<sub>4</sub> nanoparticles to yeast cells: Involvement of mitochondrial dysfunction. Chem. Biol. Interact. 2018; 287: 20-6.
  39. Luna-Vázquez-Gómez R, Arellano-García ME, García-Ramos JC, Radilla-Chávez P, Salas-Vargas DS, Casillas-Figueroa F, *et al.* Hemolysis of human erythrocytes by Argovit™ AgNPs from healthy and diabetic donors: An *in vitro* study. Materials. 2021; 14(11): 2792.

**Cite this article:** Shekhar R, Prakash HS, Geetha N. Phytofabrication of Magnetite Nanoparticles from *Piper betle* (L.) var. Mysore and Evaluation of Anti-Breast Cancer Potentials. Indian J of Pharmaceutical Education and Research. 2026;60(2s):s533-s540.